

Received: 10 January 2024

Accepted: 30 May 2024

## Synthesis and Characterization of ZnO/Cu<sub>2</sub>O and Co co-doped Ag-ZnO/Cu<sub>2</sub>O Nanoparticles with Possible Photovoltaic Applications

Kariyawasam, M. I.<sup>1</sup> & Hewage, J. W.<sup>2</sup>

malka.kariyawasam@gmail.com, jinasena@chem.ruh.ac.lk

<sup>1</sup>Department of Chemistry, Faculty of Science, University of Ruhuna, Sri Lanka.

<sup>2</sup>School of Applied Sciences, Dickinson State University, ND 58601, USA.

### Abstract

The Photovoltaics phenomenon is one of the major turning points in the battle against the depletion of fossil fuels. Sunlight is the main resource in photovoltaics, but there remains a quest to harvest it efficiently to generate electricity. This study is focused on designing basic, cost-effective prototype solar cells using ZnO/Cu<sub>2</sub>O nanoparticles (NPs) and Co(cobalt) co-doped Ag-ZnO/Cu<sub>2</sub>O NPs under normal university laboratory conditions. ITO-coated glass was used as the substrate of the solar cell and a modified low-temperature chemical bath deposition method was used for fabrication. Both ZnO and Cu<sub>2</sub>O NPs were synthesized by aqueous precipitation methods and the fabrication was performed successfully using ZnO and Cu<sub>2</sub>O NPs. However, the fabrication with Co co-doped Ag-ZnO and Cu<sub>2</sub>O NPs requires more research since the Co co-doped Ag-ZnO NPs were synthesized by solvothermal method, and it appeared as a fine powder which was not thick enough to hold onto the Cu<sub>2</sub>O layer. The UV-spectroscopic analysis confirmed the characteristic band of ZnO NPs at 367.5 nm, Cu<sub>2</sub>O NPs at 360 nm, and Co co-doped Ag-ZnO NPs at 378 nm. The FTIR spectrum showed sharp peaks at 460 cm<sup>-1</sup> and 606 cm<sup>-1</sup> for the corresponding Zn-O bond and Cu-O bond, respectively with a broad peak at 1329 cm<sup>-1</sup> for Cu<sub>2</sub>O FTIR, due to the chemisorbed and/or physisorbed H<sub>2</sub>O and CO<sub>2</sub> molecules on the surface of the nanostructure. The EDX analysis showed the presence of slight carbon impurity in ZnO NPs which resulted in a deviated XRD pattern while Cu<sub>2</sub>O NPs showed the characteristic XRD pattern. The solar cell illuminated under three different lux conditions, had the characteristic J-V plot when measured through Gamry Potentiostat.

**Keywords:** Co co-doped Ag-ZnO NPs, Cu<sub>2</sub>O NPs, Photovoltaics, solar cell, ZnO NPs.

## Introduction

Solar energy is the most abundant, out of all renewable energy sources, which can even be harnessed in cloudy weather conditions (United Nations, 2022). Currently solar energy accounts only around 1% of global electricity generation and authorities should focus more on solar energy as it will help to overcome problems associated with fossil fuels such as their obvious depletion and global warming (Abdu & Musa, 2011). The sun, which has a reasonably stable lifetime with a projected constant radiative energy output of over 10 billion years, emits solar energy primarily as electromagnetic radiation (Abdu & Musa, 2011). A solar cell absorbs this radiation and generates charge carriers via photogeneration in a light-absorbing material and separates those charge carriers to the conductive band that will transmit electricity (Abdu & Musa, 2011). This whole process is known as, the photovoltaic (PV) effect. In its rudimentary form, the solar cell consists of a junction formed between n-type and p-type semiconductors, either of the same material i.e. homojunction, or different materials i.e. Schottky or heterojunction (Abdu & Musa, 2011).

For many decades inorganic materials such as silicon dominated as the main material in building conventional solar cells (Günes & Sariciftci, 2008). Although the efficiency of such conventional solar cells is indeed high, those solar cells require very expensive materials and energy-intensive processing techniques (Günes & Sariciftci, 2008). To overcome those limitations, solution-processed solar cells based on inorganic semiconductors which include nanostructured solar cells have

emerged (Günes & Sariciftci, 2008). The main advantages of inorganic semiconductor NPs are, that they offer the benefit of having high absorption, coefficient, and size tunability (Günes & Sariciftci, 2008). By varying the size of the NPs, the bandgap can be tuned, therefore the absorption range can be tailored (Günes & Sariciftci, 2008). Furthermore, compared with organic NPs, inorganic NPs are non-toxic, hydrophilic, biocompatible, and highly stable (Paul and Sharma, 2010). According to the study of Denet (2021) the two main types of semiconductor NPs used are ZnO & Cu<sub>2</sub>O NPs because ZnO/Cu<sub>2</sub>O materials are highly abundant, cheaper, and non-toxic to humans. Furthermore, ZnO/Cu<sub>2</sub>O are natural n-type and p-type semiconductors respectively (Denet, 2021).

As mentioned above these solar cell designing methods require sophisticated fabrication techniques such as spray pyrolysis and reactive ion etching (RIE). Thus, this project works on developing advanced materials under several parallel research projects by especially focusing on the following objectives: preparation of ZnO, Co co-doped Ag-ZnO, and Cu<sub>2</sub>O NPs, developing a simple, cost-effective fabrication technique to fabricate NPs on a conductive glass under normal university laboratory conditions and checking the functionality of the fabricated solar cell from a current density vs. potential plot (J-V plot) under dark and illuminated conditions.

## Materials and Methods

Zn(CH<sub>3</sub>COO)<sub>2</sub>·2H<sub>2</sub>O (zinc acetate dihydrate) and AgNO<sub>3</sub> (silver nitrate) were obtained from BDH company. NaOH (sodium hydroxide), Cu(NO<sub>3</sub>)<sub>2</sub>·3H<sub>2</sub>O (copper(II) nitrate trihydrate), and Co(NO<sub>3</sub>)<sub>2</sub>·6H<sub>2</sub>O (cobalt(II) nitrate hexahydrate) were obtained from Merck Specialities (Pvt) Ltd. C<sub>2</sub>H<sub>2</sub>O<sub>4</sub>·2H<sub>2</sub>O (oxalic acid dihydrate) was obtained from Himedia Laboratories (Pvt) Ltd. PEG 400 (polyethylene glycol 400) was obtained from Alpha Chemika company. d-(+)-glucose anhydrous was obtained from Fluka Chemika company. All chemicals were supplied in GPR grade and were used as received without further purification.

### Preparation of ZnO NPs

The present work adopted the procedure followed by Halanayake et al (2021) for ZnO NPs preparation. 50.00 mL of 0.5 M of Zn(CH<sub>3</sub>COO)<sub>2</sub>·2H<sub>2</sub>O (5.4875 g) solution was added to a 250 mL beaker followed by 50.00 mL of 2 M NaOH (4.0000 g) to maintain the pH at 12 and stirred continuously for 2 hours by magnetic stirrer maintaining the temperature at 60 °C. The precipitate was washed three times, each with distilled water and ethanol and finally, it was dried in an oven at 60 °C for 24 hours.

### Preparation of Cu<sub>2</sub>O NPs

The procedure followed by Amini et al (2018) was adopted to prepare Cu<sub>2</sub>O NPs for the present work. A 1:1 mixture of distilled water and ethanol (each 30 mL) was mixed with Cu(NO<sub>3</sub>)<sub>2</sub>·3H<sub>2</sub>O (1.9328 g) and PEG 400 (1 mL) and stirred vigorously in a magnetic

stirrer until it dissolved completely. Then a 20 mL solution of NaOH (2.8000 g) and d-(+) glucose anhydrous (2.4 g) was slowly added dropwise under vigorous magnetic stirring to the solution. Including the time of addition of NaOH and glucose mixture, the solution was stirred for 20 minutes. Upon addition of NaOH and glucose mixture, the Cu(NO<sub>3</sub>)<sub>2</sub>·3H<sub>2</sub>O solution undergoes a serious colour change from light blue to dark blue to green and ultimately to red. Finally, the dark red precipitate was filtered, washed three times, each with distilled water and ethanol, and dried under air at room temperature, overnight.

### Preparation of Co co-doped Ag-ZnO NPs

The procedure presented by Subash et al (2013) was modified to prepare Co co-doped Ag-ZnO NPs. An aqueous solution of 0.4 M zinc acetate dihydrate was prepared by dissolving 17g of 98.5 % zinc acetate dihydrate in 200 mL of deionized water in a 500 mL beaker. At the same time, an aqueous solution of 0.6 M oxalic acid was prepared by dissolving 15 g of oxalic acid in 200 mL of deionized water in a 500 mL beaker. Then both solutions were heated separately to their boiling points. An aliquot of 10 mL of (7.500 × 10<sup>-5</sup> M) silver nitrate solution was added to the boiling zinc acetate solution and was stirred well using a glass rod. The boiled oxalic acid solution was added to the mixture of silver nitrate and zinc acetate solution portion-wise and was mixed well with a glass rod. A white precipitate of Ag-zinc oxalate (mixture A) was deposited at the bottom of the beaker. An amount of 0.3360 g of cobalt(II) nitrate hexahydrate was dissolved in 10 mL of deionized water. Then it was added to the Ag-zinc oxalate

mixture (mixture A) and was stirred well (mixture B). Then mixture B was heated for 1 hour at 60-70 °C while stirring. After that, leave the solution to be cooled to room temperature. As a result, a fine uniform precipitate of cobalt with Ag-zinc oxalate was formed. These Co/Ag-zinc oxalate crystals were washed a few times with distilled water, air-dried overnight, and dried at 100 °C for 5 hours. After that, the sample was calcined in a muffle furnace at 500 °C for 6 hours. Then the furnace was allowed to cool to room temperature. The Co co-doped Ag-ZnO catalyst was collected and weighed out. Then again calcined in the muffle furnace for 3 hours and confirmed whether the weight was constant, and no more zinc oxalate was left.

#### **Fabrication and illumination of solar cell**

Both ZnO and Cu<sub>2</sub>O NPs were fabricated on a conductive glass substrate, by using a modified, low-temperature chemical bath deposition method. A commercially available indium tin oxide (ITO) glass with dimensions of 5 cm in length and 1 cm in width, was used as the substrate. The prepared substrate was first rinsed in acetone followed by ethanol and finally with deionized water. After that, 1 cm<sup>2</sup> area from one end of the glass substrate was taped using a masking tape to a thickness of around 1 mm on a Petri dish. Then, the prepared ZnO NPs were deposited on the conductive side of the glass substrate up to 1 mm thickness avoiding the taped area. The deposition of ZnO NPs on the glass substrate was done as follows. First, the ZnO NPs were heated to boiling in a 100 mL beaker, by a Bunsen burner, with a minimal amount of distilled water to make a paste. Then the paste was poured onto a glass substrate up to the

thickness of the masking tape (1 mm) and was spread evenly by a micro spatula. After that, the petri dish containing the glass substrate and ZnO NPs was kept on a hot plate at 60 °C temperature for 15 minutes. During the ZnO NP solidification process, the thickness of the masking tape was increased with, around 0.5 mm. Soon after the ZnO layer solidifies, the Cu<sub>2</sub>O NPs paste was prepared and fabricated following the same procedure for ZnO NPs fabrication. After that, the glass substrate containing both ZnO and Cu<sub>2</sub>O was kept at 60 °C for 15 minutes for the solidification of the Cu<sub>2</sub>O layer. The temperature and the time should always be controlled carefully, else the ZnO NPs layer and Cu<sub>2</sub>O NPs layer will get cracked and the Cu<sub>2</sub>O NPs layer might leak into the conductive glass layer. The cracking and leaking of layers will result in the dysfunction of the solar cell. Finally, the solar cell was illuminated by one zero technology, SL-838 dimmable table lamp under three different lux conditions.

#### **Results and Discussion**

##### **Characterization of ZnO NPs and Co co-doped Ag-ZnO NPs**

A wavelength scan was carried out on the range 300-400 nm for ZnO NPs and Co co-doped Ag-ZnO NPs using the UH5300 Hitachi spectrophotometer. The literature UV data for ZnO NPs is reported as 364 nm and 374 nm at pH 12 (Halanayake et al, 2021, Jay Chithra et al, 2015). As shown in Figure 1, since the value obtained from this study, which is 367.5 nm, is in the range between 364 nm and 374 nm, the prepared ZnO can be considered as NPs (Halanayake et al., 2021, Jay Chithra et al., 2015). The EDX spectrum of ZnO NPs

shown in Figure 2 displays that prepared NPs contain a slight impurity of carbon.

**Figure 1.**

*The UV-vis spectrum of ZnO NPs.*

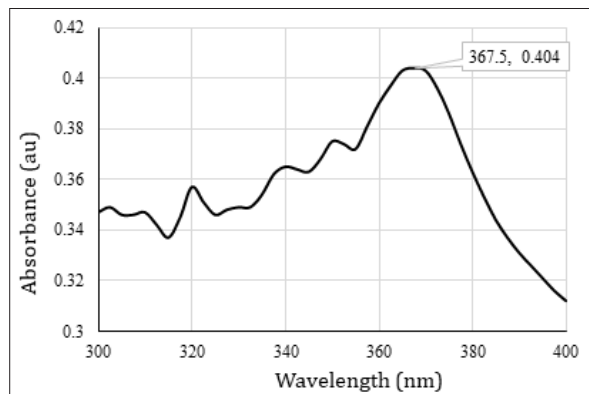
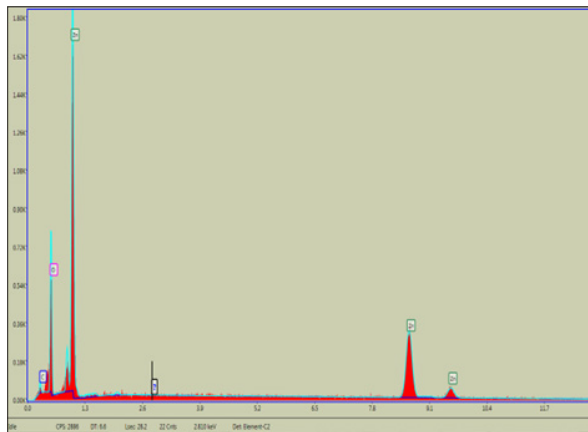


**Figure 2.**

*The EDX spectrum of ZnO NPs.*



The XRD of the present study of ZnO NPs which is shown in Figure 3 from 10-80 2(theta)-angle range (covered by the rectangular area) agrees with the literature XRD patterns (Halanayake et al, 2021, Jay Chithra et al, 2015). The ‘d’ values 2.81164 Å, 2.60825 Å, 2.47679 Å, 1.91304 Å, 1.62615 Å, 1.47823 Å, 1.40908 Å, 1.38005 Å, and 1.36184 Å of the graph correspond to XRD miller indices (100), (002), (101), (102), (110), (103), (200), (112), (201) respectively, which are also reported in the literature (Halanayake

et al., 2021; Jay Chithra et al., 2015). The major peak between 5-10 2(theta)-angle can be accounted for carbon impurity. The FTIR data shown in Figure 4 is in close agreement with the literature values (Jay Chithra et al., 2015; Oprea et al., 2011). The deviation from the literature range can be concluded as the presence of carbon impurity.

**Figure 3.**

*The XRD spectrum of ZnO NPs.*

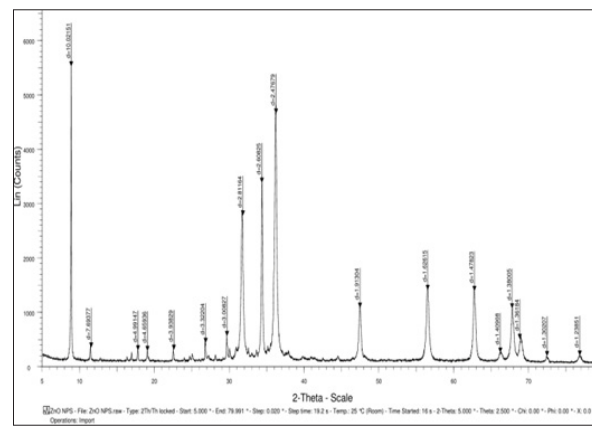
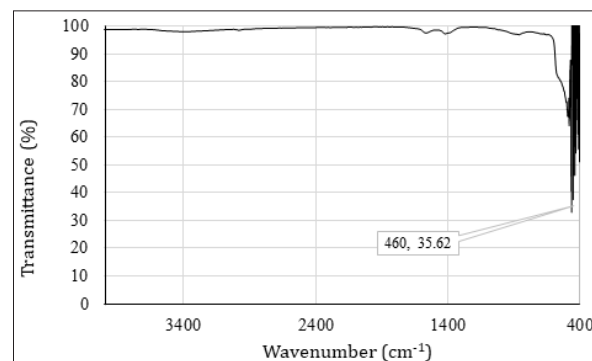


**Figure 4.**

*The FTIR spectrum of ZnO NPs.*



The SEM image shown in the 200 nm range in Figure 5 confirms the formation of ZnO NPs (Halanayake et al., 2021). As shown in Figure 6, the current study shows a 378 nm peak for the Co co-doped Ag-ZnO NPs. The shifting of  $\lambda_{max}$  from 367.5 nm to 378 nm proves that the doping was successful. Thus, the band gap

has been reduced paving the way to increased photovoltaic efficiencies.

**Figure 5.**

*The SEM image of ZnO NPs.*

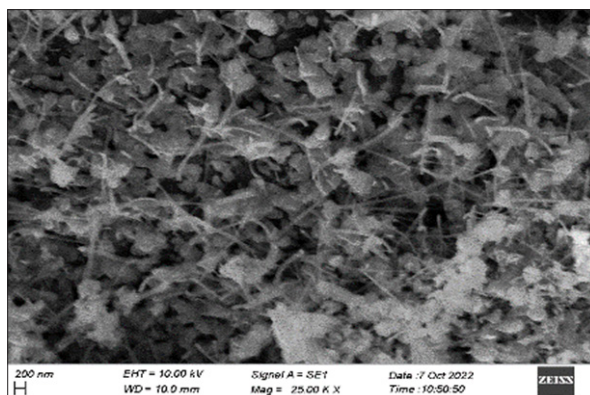
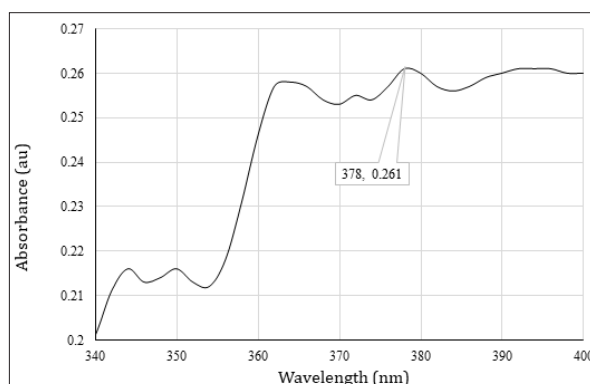


**Figure 6.**

*The UV-vis spectrum of Co co-doped Ag-ZnO NPs.*



### Characterization of Cu<sub>2</sub>O NPs and J-V plot for ZnO/Cu<sub>2</sub>O solar cell

As shown in Figure 7, a wavelength scan was carried out on the range 300-750 nm for Cu<sub>2</sub>O NPs using UH5300 Hitachi spectrophotometer. An increase in intensity at 360 nm indicated the presence of Cu<sub>2</sub>O NPs while a decrease in intensity at 360 nm indicated the presence of CuO NPs (Butte & Waghuley, 2020, Zhang et al., 2010). The current study indicates an increase in intensity at 360 nm. Therefore, the UV data obtained from the current study

is in good agreement with the literature values (Butte & Waghuley, 2020). The EDX spectrum of Cu<sub>2</sub>O NPs in Figure 8 shows that there are only Cu and O in the sample proving that the prepared Cu<sub>2</sub>O NPs are pure.

**Figure 7.**

*The UV-vis spectrum of Cu<sub>2</sub>O NPs.*

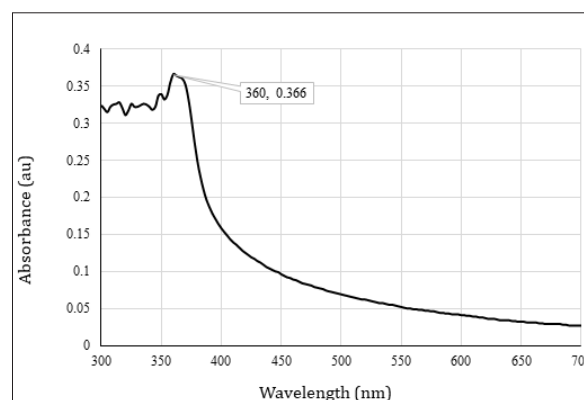
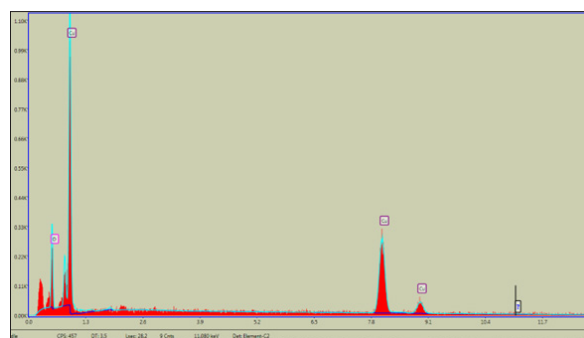


**Figure 8.**

*The EDX spectrum of Cu<sub>2</sub>O NPs.*



The XRD spectra of Cu<sub>2</sub>O NPs of the current study which is shown in Figure 9, correspond with the literature XRD patterns (Amini et al, 2018). The 'd' values 3.03258 Å, 2.47278 Å, 2.13686 Å, 1.50984 Å, 1.28631 Å, and 1.23194 Å of the graph correspond to XRD miller indices (110), (111), (200), (220), (311), (222) respectively, which were also reported in the literature (Amini et al, 2018). The literature stated typical Cu-O stretching of Cu<sub>2</sub>O NPs was in the range of 601-624 cm<sup>-1</sup> (Zhang et al., 2010, Joshi et al., 2016).

Hence, the FTIR data shown in Figure 10 for prepared Cu<sub>2</sub>O NPs are in good agreement with the literature value range. The broad absorption band between 1300 and 2000 cm<sup>-1</sup> was mainly assigned to the chemisorbed and/or physisorbed H<sub>2</sub>O and CO<sub>2</sub> molecules on the surface of the nanostructure (Winkler et al, 2018).

**Figure 9.**  
*The XRD spectrum of Cu<sub>2</sub>O NPs.*

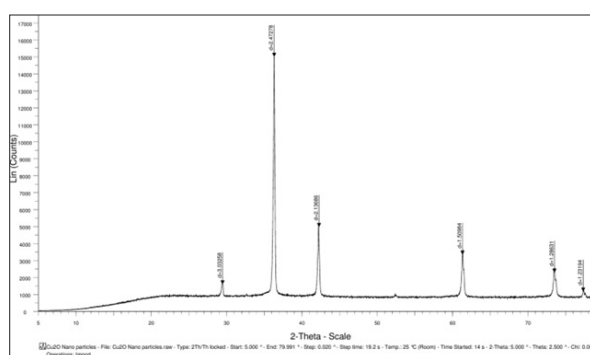
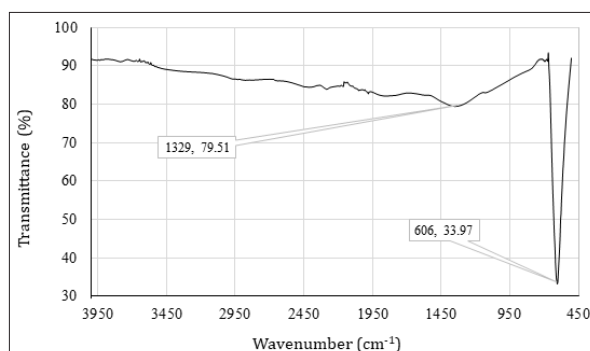


**Figure 10.**  
*The FTIR spectrum of Cu<sub>2</sub>O NPs.*



The SEM image of Cu<sub>2</sub>O NPs shown in the 200 nm range in Figure 11 confirms the formation of NPs and they are in good agreement with the literature images (Amini et al., 2018). The current density vs potential plot (J-V plot) of the present study in Figure 12 follows the typical J-V curve for solar cells (Winkler et al, 2018, Cui and Gibson, 2010). This concludes that the designed ZnO/Cu<sub>2</sub>O solar cell is functioning.

**Figure 11.**  
*The SEM image of Cu<sub>2</sub>O NPs.*

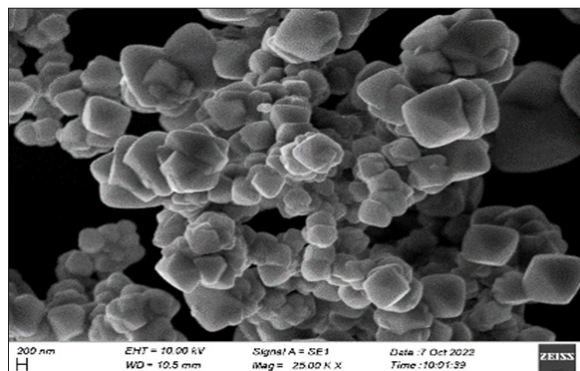
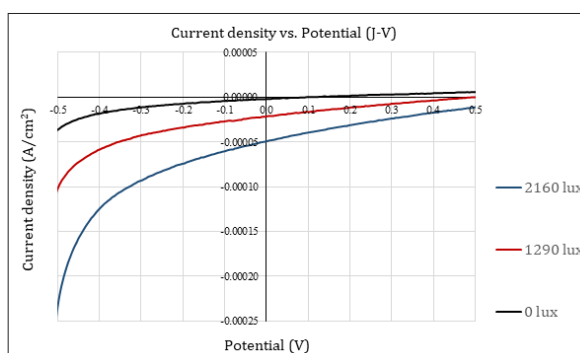


**Figure 12.**  
*The J-V plot of ZnO/Cu<sub>2</sub>O cell.*



## Conclusions

The ZnO, Co co-doped Ag-ZnO and Cu<sub>2</sub>O NPs were successfully prepared and characterized. The  $\lambda_{\text{max}}$  378 nm of Co co-doped Ag-ZnO confirms the reduction of the band gap of doped ZnO which leads the path to increased photovoltaics efficiencies of ZnO. The solar cell fabricated with ZnO/Cu<sub>2</sub>O demonstrated the typical J-V plot, which confirms the successfulness of the fabrication technique and ultimately the prepared solar cell. Additionally, an attempt to prepare a more efficient solar cell fabricated with Co co-doped Ag-ZnO and Cu<sub>2</sub>O was made. Since the Co-co-doped Ag-ZnO NPs appeared like a very fine powder due to calcining at 500 °C, the Co-co-doped Ag-ZnO layer was not thick

enough to hold and as a result the fabrication was unsuccessful. A study by Cui and Gibson (2010) involves a concept called nanopillars to strengthen nanoparticle layers which can be inculcated in future studies. A method can be developed to hold together Co co-doped Ag-ZnO NPs firmly to the substrate.

### Acknowledgment

My appreciation goes to the Department of Chemistry, University of Ruhuna for providing me with the necessary facilities to complete my research.

### References

- Abdu, Y. and Musa, A. (2011). Copper (I) oxide (Cu<sub>2</sub>O) based solar cells - a review. *Bayero Journal of Pure and Applied Sciences*, 2(2). <https://doi.org/10.4314/bajopas.v2i2.63717>.
- Amini, M., Ramezani, S., Anbari, A. P., Beheshti, A., Gautam, S., & Chae, K. H. (2018). Simple Preparation of Cuprous Oxide Nanoparticles for Catalysis of Azide-alkyne Cycloaddition. *Journal of Chemical Research*, 42(3), 166–169. <https://doi.org/10.3184/174751918x15221562069666>.
- Butte, S. M., & Waghuley, S. A. (2020). Optical properties of Cu<sub>2</sub>O and CuO. *AIP Conference Proceedings*. <https://doi.org/10.1063/5.0001644>.
- Cui, J., & Gibson, U. J. (2010). A Simple Two-Step Electrodeposition of Cu<sub>2</sub>O/ZnO Nanopillar Solar Cells. *The Journal of Physical Chemistry C*, 114(14), 6408–6412. <https://doi.org/10.1021/jp1004314>.
- Denet, C. (2021). Análisis y diseño de un dispositivo optoelectrónico basado en capas finas de CuO/ZnO obtenido por electrodeposición. *Riunet.upv.es*. <https://riunet.upv.es/handle/10251/163254#>.
- Günes, S. and Sariciftci, N. S. (2008). Hybrid Solar Cells. *Inorganica Chimica Acta*, 361 (3), 581–588. <https://doi.org/10.1016/j.ica.2007.06.042>.
- Halanayake, K. D., Kalutharage, N. K., & Hewage, J. W. (2021). Microencapsulation of biosynthesized zinc oxide nanoparticles (ZnO-NPs) using Plumeria leaf extract and kinetic studies in the release of ZnO-NPs from microcapsules. *SN Applied Sciences*, 3(1). <https://doi.org/10.1007/s42452-020-04100-3>.
- Jay Chithra, M., Sathya, M., & Pushpanathan, K. (2015). Effect of pH on Crystal Size and Photoluminescence Property of ZnO Nanoparticles Prepared by Chemical Precipitation Method. *Acta Metallurgica Sinica (English Letters)*, 28(3), 394–404. <https://doi.org/10.1007/s40195-015-0218-8>.
- Joshi, S., Ippolito, S. J., & Sunkara, M. V. (2016). Convenient architectures of Cu<sub>2</sub>O/SnO<sub>2</sub> type II p–n heterojunctions and their application in visible light catalytic degradation of rhodamine B. *RSC Advances*, 6(49), 43672–43684. <https://doi.org/10.1039/c6ra07150c>.



- Oprea, O., Andronescu, E., Vasile, B., Voicu, G., & Covaliu, C. (2011). Synthesis and Characterization of ZnO nanopowder by non- basic route. *Digest Journal of Nanomaterials and Biostructures*, 6, 1393–1401. [https://chalcogen.ro/1393\\_Oprea.pdf](https://chalcogen.ro/1393_Oprea.pdf).
- Paul, W., & Sharma, C. P. (2010). Inorganic nanoparticles for targeted drug delivery. *Biointegration of Medical Implant Materials*, 204–235. <https://doi.org/10.1533/9781845699802.2.204>.
- Subash, B., Krishnakumar, B., Swaminathan, M., & Shanthi, M. (2013). Highly Efficient, Solar Active and Reusable Photocatalyst: Zr-Loaded Ag–ZnO for Reactive Red 120 Dye Degradation with Synergistic Effect and Dye-Sensitized Mechanism. *Langmuir*, 29(3), 939–949. <https://doi.org/10.1021/la303842c>.
- United Nations. (2022). What Is Renewable energy? United Nations; United Nations. <https://www.un.org/en/climatechange/what-is-renewable-energy>.
- Winkler, N., Edinger, S., Kaur, J., Wibowo, R. A., Kautek, W., & Dimopoulos, T. (2018). Solution-processed all-oxide solar cell based on electrodeposited Cu<sub>2</sub>O and ZnMgO by spray pyrolysis. *Journal of Materials Science*, 53(17), 12231–12243. <https://doi.org/10.1007/s10853-018-2482-2>.
- Zhang, X., Song, J., Jiao, J., & Mei, X. (2010). Preparation and photocatalytic activity of cuprous oxides. *Solid State Sciences*, 12(7), 1215–1219. <https://doi.org/10.1016/j.solidstatesciences.2010.03.009>.